PHYSICAL REVIEW E VOLUME 56, NUMBER 1 JULY 1997

ARTICLES

Soluble phase field model

Umberto Marini Bettolo Marconi
Dipartimento di Matematica e Fisica, Università di Camerino, Via Madonna delle Carceri, I-62032, Camerino, Italy; INFM, Unità di Camerino, Camerino, Italy; and INFN, Unità di Perugia, Perugia, Italy

Andrea Crisanti and Giulia Iori
Dipartimento di Fisica, Università di Roma ''La Sapienza,'' Piazzale Aldo Moro 2, I-00185, Roma, Italy and INFM, Unità di Roma I, Roma, Italy

(Received 27 December 1996)

The kinetics of an initially undercooled solid-liquid melt is studied by means of a generalized phase field model, which describes the dynamics of an ordering nonconserved field ϕ (e.g., solid-liquid order parameter) coupled to a conserved field (e.g., thermal field). After obtaining the rules governing the evolution process, by means of analytical arguments, we present a discussion of the asymptotic time-dependent solutions. The full solutions of the exact self-consistent equations for the model are also obtained and compared with computer simulation results. In addition, in order to check the validity of the present model we compare its predictions with those of the standard phase field model and found reasonable agreement. Interestingly, we find that the system relaxes towards a mixed phase, depending on the average value of the conserved field, i.e., on the initial condition. Such a phase is characterized by large fluctuations of the ϕ field. [S1063-651X(97)05505-0]

PACS number(s): 64.60.Cn, 64.60.My, 64.60.Ak

INTRODUCTION

In the past few years considerable effort has been devoted to the study of systems far from equilibrium [1]. Well-known examples are provided by phase separating systems, initially prepared in a state of equilibrium, and rendered unstable by modifying a control parameter such as temperature, pressure, or magnetic field. To restore stability they evolve towards a different equilibrium state determined by the final value of the controlling fields. Such evolution can be very slow and is often characterized by nonuniform, complex structures in both space and time.

Two simple dynamical models, often called model *A* [2] and model *B* [3], have been introduced in the literature in order to understand kinetic ordering phenomena (see also [4,5]). Model *A* describes the growth process, when the order parameter is nonconserved, whereas model *B* is appropriate if the order parameter is conserved. In the first case, the late stage growth is driven by the tendency of the system to minimize the energy cost due to the presence of interfaces between regions separating different phases. Thus, as the curvature decreases the process slows down and the domain size $L(t)$ grows in time according to the law $L(t) \sim t^{1/2}$. In the conserved case, the approach to equilibrium is limited by the diffusion of the aggregating material, as larger domains can grow only at the expense of smaller ones. The average size $L(t)$ increases proportionally to $t^{1/z}$, where the dynamical exponent z is 3 for scalar order parameters and 4 for vector order parameters.

Another model, known as the phase field model (PFM), is somehow intermediate between *A* and *B* and consists of two fields coupled bilinearly: one field represents a nonconserved ordering parameter, with type-*A* dynamics, whereas the second is a temperature shift field subject to a diffusion equation supplemented by a source term. The model can be cast in the form of coupled partial differential equations for a nonconserved order parameter interacting with a time-dependent conserved field. Its dynamics is very rich since it displays features characterizing both the pure *A* and the pure *B* models as it is revealed from the analysis of the structure functions at different times. In other words, after a rapid initial evolution one observes an intermediate stage in which the growth is curvature driven and an asymptotic regime during which diffusion-limited behavior is seen.

The PFM, introduced and physically motivated by Langer [6] provides a theoretical framework for many natural processes. It is designed to treat situations where the relaxation dynamics of the order parameter associated with the presence of a liquid or a solid is coupled to the diffusion of heat released during the change of state.

An example is the growth of a solid nucleus from its undercooled melt, a phenomenon encountered in rapidly solidifying materials, such as metals, where the growth is limited by the rate of transport of the heat of fusion away from the solid-liquid boundary [7]. As the heat released by the solid accumulates at the interface, it slows down the growth because diffusion must act over a thicker and thicker region. This mechanism has implications also in the morphology of the growing phases and is responsible for the instability of a planar solid-liquid interface with respect to a perturbation of its shape; one realizes immediately that a protrusion of the solid phase into the liquid advances faster than its neighboring regions because it explores a region where the undercooling is greater, so its growth becomes faster. The solid-liquid surface tension eventually provides the necessary balance and prevents the interface from being eroded by fluctuations

1063-651X/97/56(1)/77(11)/$10.00

of very short wavelength [8,9].

Another very closely related problem is the growth of the solid phase in multicomponent solutions, where one of the components is to be diffused away from the interface in order to form a stable crystal [7]. In the present paper, we shall confine the discussion to the thermal case for the sake of clarity and investigate the kinetic ordering of a spherical version of the phase field model. This study extends our previous investigations [10–12] to include a nonvanishing order parameter. In our opinion it can be useful because it provides the few models whose static properties can be obtained exactly in arbitrary dimensionality and whose relaxation behavior can be analyzed in great detail by means of analytical and numerical methods. We note that in the field of ordering kinetics there exist only a few models for which the relaxation can be studied without performing extensive numerical calculations. In particular the late-stage behavior of processes with conserved dynamics is hardly observable numerically due to computer limitations [12,13]. Besides the examples cited above, this study may be of some help in treating analytically some models introduced recently with the aim of describing irreversible aggregation phenomena [14].

In the present paper we generalize the model, introduced previously by two of us [10,11], to the case of off-critical quenches, e.g., to initial conditions corresponding to nonvanishing values of the fields. The structure of the paper is the following. In order to make the paper self-contained we have included two sections (I and II) where we recall some basic notions, which lead to the thermodynamic derivation of the phase field model [6,15–17] and the construction of the Lyapunov functional, from which the coupled equations of motion of the PFM can be derived. In Sec. III we state the spherical phase field model and write explicitly the closed set of equations, which we discuss qualitatively in Sec. IV. In Sec. V comparisons with numerical simulations in $d=2$ at zero temperature are illustrated. The predictions of the spherical model are compared with those of a more realistic scalar order parameter phase field model and the similarities and differences are stressed in the Conclusion.

I. THERMODYNAMIC PRELIMINARIES

Let us consider a material that under suitable conditions of pressure and temperature can exist in two distinct thermodynamic phases: a liquid and a solid. If the pressure is held constant at the value corresponding to solid-liquid equilibrium and the temperature T is varied one can favor the solid phase for $T<T_M$ or the liquid phase for $T>T_M$, where T_M is the melting temperature at which the equilibrium first-order transition takes place. One usually calls an undercooled melt a material brought below its melting temperature, but still in the liquid phase.

We shall consider the situation $T<T_M$, which is experimentally and technologically more interesting. Below T_M the value of the thermodynamic Gibbs potential of the solid phase is lower than that of the liquid phase, which is only metastable. A convenient way of studying the solidification process is to adopt a phenomenological Ginzburg-Landau description by introducing a suitable crystalline order parameter ϕ, which assumes the conventional value ϕ_l in the liquid phase and ϕ_s in the solid phase. One then employs a field-theoretic free-energy functional of the form

$$F[\phi]=\epsilon\int d^dx\left[\frac{\xi^2}{2}(\nabla\phi)^2+f(\phi)\right], \tag{1}$$

where $f(\phi)$ is a function of the order parameter ϕ with the property of having two minima of equal depth at $\phi=\phi_l$ and $\phi=\phi_s$.

The constant ϵ has dimensions of energy over volume and is for the moment arbitrary. The gradient term represents the energy cost necessary to create an inhomogeneity in the system and the quantity ξ has the dimension of length and is associated with the scale over which an inhomogeneity in the system vanishes. Upon minimizing $F[\phi]$ with respect to ϕ and selecting the nonuniform localized solution of the variational Euler-Lagrange equation corresponding to the lowest value of the Gibbs free energy one obtains the surface tension σ of the model, which is proportional to the correlation length

$$\sigma\sim\epsilon\xi \tag{2}$$

and thus to the interface thickness. The numerical coefficient is of order 1 and will be ignored because it does not influence our discussion.

In order to include undercooling or overheating effects, i.e., a temperature different from T_M, we introduce a dimensionless field

$$u(\boldsymbol{x})=\frac{c_p}{L}[T(\boldsymbol{x})-T_M] \tag{3}$$

proportional to the local temperature shift $[T(x)-T_M]$. The constants c_p and L are, respectively, the specific heat at constant pressure and the latent heat of fusion per unit volume. The local field u acts as an external field, conjugate to the crystalline order parameter ϕ, favoring the solid phase for $u<0$ and the liquid phase for $u>0$. For $u=0$ the two phases coexist.

As usually done for a first-order phase transition, metastability is taken into account by eliminating ϕ in favor of u via a Legendre transform. One then introduces the Gibbs potential

$$G[u]=F[\phi]-\lambda\epsilon\int d^dx\ u(\boldsymbol{x})\phi(\boldsymbol{x}), \tag{4}$$

where $\phi=\phi[u]$ is obtained from

$$\frac{\delta F[\phi]}{\delta\phi(x)}=\lambda\epsilon u(x) \tag{5}$$

and λ is a nondimensional parameter. A convenient way to relate λ to the known thermodynamic parameters is to consider the entropy difference between the pure uniform solid ($\phi=\phi_s$) and liquid ($\phi=\phi_l$) phases at the melting temperature. This is related to the latent heat by the relation

$$S_l-S_s=\frac{LV}{T_M}, \tag{6}$$

where S_l and S_s are the entropies of the liquid phase and of the solid phase, respectively, and V is the volume of the system. By using the thermodynamic relation

$$\frac{\partial G}{\partial T} = -S, \tag{7}$$

Eq. (3), and the expression (4) for uniform fields, we get

$$\frac{LV}{T_M} = -\left.\frac{\partial G}{\partial T}\right|_{\phi_l,T_M} + \left.\frac{\partial G}{\partial T}\right|_{\phi_s,T_M} = \lambda\epsilon V(\phi_l-\phi_s)\frac{c_p}{L}, \tag{8}$$

from which we obtain

$$\lambda = \frac{L^2}{\epsilon c_p T_M \Delta\phi}, \tag{9}$$

where $\Delta\phi = \phi_l - \phi_s$.

Next consider a solid spherical drop of radius $R \gg \xi$ immersed in an undercooled melt $(u<0)$. The Gibbs potential G with the drop is [see Eq. (4)]

$$G = G_0 + \lambda\epsilon u \frac{4\pi}{3} R^3 \Delta\phi + 4\pi R^2 \sigma, \tag{10}$$

where the first term is the Gibbs potential G without the droplet, the second term is the gain in replacing the liquid with a solid in the droplet, and the third term is the cost in creating a surface separating the liquid and solid phases. In equilibrium no energy is needed to create the droplet, so G is stationary with respect to variation of R. By imposing $\delta G = 0$ we readily obtain the critical nucleation radius R_N,

$$R_N = \frac{d_0}{|u|}, \tag{11}$$

where

$$d_0 = \frac{2\sigma}{\Delta\phi\lambda\epsilon} \tag{12}$$

is a capillarity length, which, using the expression of λ, Eq. (9), can be written as

$$d_0 = \frac{2\sigma c_p T_M}{L^2}. \tag{13}$$

Finally, from Eqs. (9) and (12) it follows that we can write the dimensionless parameter λ as the ratio two length

$$\lambda = \frac{\xi}{d_0}, \tag{14}$$

where we have defined $\epsilon\,\xi = (2/\Delta\phi)\,\sigma$ [cf. Eq. (2)]. We see that λ is small provided the interfacial thickness is much shorter than the capillary length.

II. PHASE FIELD MODEL

In this section we shall introduce relaxational dynamics into the model. A large body of work in the area of dynamic phase transitions has focused on the time-dependent Ginzburg-Landau (TDGL) model because of its ability to describe a variety of problems. In equilibrium the field $\phi(\boldsymbol{x})$ minimizes the Gibbs potential G. Thus we assume that the approach to equilibrium is described by

$$\begin{aligned}\frac{\partial\phi(\boldsymbol{x},t)}{\partial t} &= -\Gamma_\phi \frac{\delta}{\delta\phi(\boldsymbol{x},t)} G[\phi,u] \\ &= -\Gamma_\phi[-\xi^2\nabla^2\phi + f'(\phi) - \lambda u],\end{aligned} \tag{15}$$

where the last equality is obtained using Eq. (4). If the field u varies on time scales much longer than those of ϕ it can be considered ''quenched'' and Eq. (15) would be the standard nonconserved TDGL equation, or model A.

In the phase field model and in the absence of external sources, $u(\boldsymbol{x},t)$ is assumed to evolve on time scales of the same order of magnitude as those of ϕ towards a homogeneous configuration. The time evolution of u is now coupled to that of ϕ and cannot be neglected anymore. In fact, when a piece of material solidifies it expels some heat and the surrounding liquid melt warms up, causing the average temperature to increase. When a region of solid melts in turn it adsorbs some heat and the liquid becomes colder.

As a consequence, Eq. (15) has to be supplemented with an equation for u. The thermal field $u(\boldsymbol{x},t)$ is subject to the Fourier equation of diffusion of heat plus an additional source term that represents the latent heat of solidification, accompanying the appearance of the solid phase.

The energy balance requires that the latent heat released at the transition equates the temperature change of the melt multiplied by the specific heat, i.e.,

$$\frac{\partial u(\boldsymbol{x},t)}{\partial t} = D\nabla^2 u(\boldsymbol{x},t) - \frac{1}{\Delta\phi}\frac{\partial\phi(\boldsymbol{x},t)}{\partial t}, \tag{16}$$

where D is the thermal diffusivity and the last term on the right-hand side is the amount of material that crystallizes per unit time and is thus proportional to the heat released during the first-order transition [6]. The coefficient $\Delta\phi$ guarantees the correct energy balance. Notice that the last term represents a source of heat when $\partial\phi(\boldsymbol{x},t)/\partial t$ is negative, i.e., when the system solidifies, or a sink when it melts, for positive $\partial\phi(\boldsymbol{x},t)/\partial t$. In other words, since we are considering a closed system the total amount of solid produced is proportional to the change of the average temperature of the system.

The two dynamical equations (15) and (16) can be obtained from a unique Lyapunov functional $\mathcal{F}$, which plays the role of the time-dependent Ginzburg-Landau potential in the present problem. In order to establish the form of $\mathcal{F}$ we perform the transformation

$$U = u + \frac{\phi}{\Delta\phi} \tag{17}$$

and eliminate u in favor of the new field U. One can then write Eqs. (15) and (16) as

$$\frac{\partial\phi(\boldsymbol{x},t)}{\partial t} = -\Gamma_\phi \left.\frac{\delta\mathcal{F}}{\delta\phi(\boldsymbol{x},t)}\right|_U, \tag{18}$$

$$\frac{\partial U(\boldsymbol{x},t)}{\partial t} = D\,\nabla^2 \left.\frac{\delta\mathcal{F}}{\delta U(\boldsymbol{x},t)}\right|_\phi, \tag{19}$$

with the Lyapunov functional [13,12]

$$\mathcal{F}[\phi,U]=\int d^dx\left[\frac{\xi^2}{2}(\nabla\phi)^2+f(\phi)+\frac{\lambda\Delta\phi}{2}\left(U-\frac{\phi}{\Delta\phi}\right)^2\right]. \tag{20}$$

Note that the dynamics of U is conserved. When the temperature field vanishes, i.e., $U=\phi/\Delta\phi$, the functional $\mathcal{F}$ has two equivalent minima, corresponding to two spatially uniform solutions: the uniform solid and liquid phases. In general, Eqs. (18)–(20) generate a complex dynamical behavior that has been the object of some studies.

In the long-time limit we may expect that while u becomes homogeneous, the crystalline field ϕ roughly assumes only the two values ϕ_l and ϕ_s. If this is the case, from the knowledge of U and u we can compute the fraction of volume occupied by the two phases. Indeed, we can write $\overline{\phi}=x_s\phi_s+x_l\phi_l$, where x_s and x_l are the fractions of volume occupied by the solid and liquid phases, respectively, and the overbar denotes spatial average. From Eq. (17) and the condition $x_s+x_l=1$, we get

$$x_l=-\frac{\phi_s}{\Delta\phi}+\overline{U}-\overline{u},\quad x_s=\frac{\phi_l}{\Delta\phi}-\overline{U}+\overline{u}, \tag{21}$$

where $\overline{u}\simeq u$ is the asymptotic value and $\overline{U}$ is the initial value its dynamics being conserved. From this it follows that if the asymptotic value of u is zero, i.e., the system relaxes towards a two-phase coexistence, the fraction of volume occupied by each phase is determined only by the initial value of $\overline{U}$. We also notice that when the system starts with an undercooling $\overline{u}=-1$ and an order parameter $m(t=0)=1$, i.e., $\overline{U}$, the latent heat produced is just enough to heat the melt at the final equilibrium temperature $\overline{u}=0$. In such a case the final volume fraction of the solid is simply $x_s=1/2-U$ and attains its maximum for $U=-1/2$.

The functional $\mathcal{F}$ decreases with time, as can be shown using Eqs. (18) and (19):

$$\begin{aligned}\frac{d\mathcal{F}}{dt}&=\int d^dx\left[\frac{\delta\mathcal{F}}{\delta\phi(\boldsymbol{x},t)}\frac{\partial\phi(\boldsymbol{x},t)}{\partial t}+\frac{\delta\mathcal{F}}{\delta U(\boldsymbol{x},t)}\frac{\partial U(\boldsymbol{x},t)}{\partial t}\right]\\&=-\int d^dx\left[\Gamma_\phi\left(\frac{\delta\mathcal{F}}{\delta\phi(\boldsymbol{x},t)}\right)^2+D\left(\frac{\nabla\delta\mathcal{F}}{\delta U(\boldsymbol{x},t)}\right)^2\right]\leqslant 0.\end{aligned} \tag{22}$$

So far we have discussed purely deterministic evolution of the order parameter and of the thermal field. Noises can be added to both equations to represent the effect of short-wavelength fluctuations; in this case Eq. (22) does not hold.

III. SPHERICAL PHASE FIELD MODEL

The choice of the local function $f(\phi)$ is somehow arbitrary, as long as the general property

$$\lim_{\phi\to\pm\infty}f(\phi)=+\infty \tag{23}$$

and two equal minima for $\phi=\phi_s$ and $\phi=\phi_l$ are satisfied. An often used form for $f(\phi)$ is

$$f(\phi)=-g\left(\frac{\phi^2}{2}-\frac{\phi^4}{4}\right), \tag{24}$$

which is even and has two equal minima at $\phi=\phi_s=-1$ and $\phi=\phi_l=1$, so that $\Delta\phi=2$. The parameter g gives the strength of the local constraint. In the limit of a large positive value of g the field ϕ can take only the values ϕ_s and ϕ_l (Ising-like variables).

The phase field model described by Eqs. (18)–(20) contains all the relevant ingredients necessary to describe the phase separation occurring in solid forming melts. However, due to the local nonlinear terms contained in the function $f(\phi)$ the solution of the dynamical equations (18)–(20) are far too difficult and are known only for some special situations. In the general case the known results follow from dimensional arguments.

To overcome this difficulty, an alternative strategy is to modify the model into a simpler one, yet maintain the general properties. This can be achieved by replacing the local quartic term in Eq. (24):

$$\int d^dx\ \phi(\boldsymbol{x})^4\to\frac{1}{V}\left[\int d^dx\ \phi(\boldsymbol{x})^2\right]^2. \tag{25}$$

This kind of constraint is much softer than Eq. (24) since it does not act on each site, but globally over the whole volume. In the following we shall denote it as a *globally constrained model* or *spherical model* [18–20], in contrast to the model (18)–(20) where the constraint is local [21,22].

The price one pays for this change is the loss of sharp interfaces between two coexisting phases. Abraham and Robert [23] showed several years ago that the spherical model in a zero external field displays two ordered phases below the critical temperature, but no phase separation. Equivalently, one can say that a planar interface between two coexisting phases is unstable due to the presence of long-wavelength excitations analogous to spin waves, an instability much stronger than the one due to the presence of capillary waves in the scalar order parameter case [24,25]. As a consequence, while this choice is very convenient for analytic calculations, it changes the structures of the nonuniform solutions in the static limit. Nevertheless, in spite of this fact, the model has a rich phenomenology, as we shall see below, and the approach to equilibrium remains highly nontrivial.

From Eqs. (20), (24), and (25) the potential $\mathcal{F}$ for the spherical model reads

$$\begin{aligned}\mathcal{F}[\phi,U]=\int d^dx\left[\frac{\xi^2}{2}(\nabla\phi)^2+\frac{1}{2}\left(\frac{\lambda}{2}-g\right)\phi^2+\lambda U^2\right.\\\left.-\lambda U\phi\right]+\frac{g}{4V}\left(\int d^dx\ \phi^2\right)^2,\end{aligned} \tag{26}$$

which, substituted into

$$\frac{\partial\phi(\boldsymbol{x},t)}{\partial t}=-\Gamma_\phi\frac{\delta}{\delta\phi(\boldsymbol{x},t)}\mathcal{F}[\phi,U]+\eta(\boldsymbol{x},t), \tag{27}$$

$$\frac{\partial U(\boldsymbol{x},t)}{\partial t}=D\nabla^2\frac{\delta}{\delta U(\boldsymbol{x},t)}\mathcal{F}[\phi,U]+\xi(\boldsymbol{x},t), \tag{28}$$

determines the time evolution of the fields ϕ and U [26]. We added to the evolution equations a noise term to simulate the effect of short-wavelength fluctuations. The two fields η and ξ are independent Gaussian fields with zero mean and two-point correlations:

$$\langle \eta(\boldsymbol{x},t)\,\eta(\boldsymbol{x}',t')\rangle = 2\,T_f\,\Gamma_\phi\;\delta(\boldsymbol{x}-\boldsymbol{x}')\,\delta(t-t'), \tag{29}$$

$$\langle \xi(\boldsymbol{x},t)\xi(\boldsymbol{x}',t')\rangle = -2\,T_f\,D\;\nabla^2\delta(\boldsymbol{x}-\boldsymbol{x}')\,\delta(t-t'), \tag{30}$$

$$\langle \eta(\boldsymbol{x},t)\xi(\boldsymbol{x}',t')\rangle = 0, \tag{31}$$

where T_f is the temperature of the final equilibrium state, whereas D and Γ_ϕ are the kinetic coefficients appearing in Eqs. (27) and (28).

It is useful to separate the spatially uniform component of fields ϕ and U. Thus introducing the Fourier component of the fields we have

$$\phi(\boldsymbol{x}) = \sum_{\boldsymbol{k}}\;\phi(\boldsymbol{k})\;e^{i\boldsymbol{k}\cdot\boldsymbol{x}},\quad \phi(\boldsymbol{k}) = (1/V)\int d^dx\;\phi(\boldsymbol{x})\;e^{-i\boldsymbol{k}\cdot\boldsymbol{x}} \tag{32}$$

and

$$\phi(\boldsymbol{k},t) = m(t)\,\delta_{k,0} + \delta\phi(\boldsymbol{k},t), \tag{33}$$

$$U(\boldsymbol{k},t) = Q(t)\,\delta_{k,0} + \delta U(\boldsymbol{k},t), \tag{34}$$

where both $\delta\phi$ and δU are zero for $k=|\boldsymbol{k}|=0$, $m(t)=\phi(t)$, and $Q(t)=U(t)$.

To study the behavior at finite temperature T_f it is also useful to introduce the equations of motion for the three equal-time real-space connected correlation functions $C_{\phi\phi}(r,t)=\langle\phi(R+r,t)\phi(R,t)\rangle_c$, $C_{\phi U}(r,t)=\langle\phi(R+r,t)U(R,t)\rangle_c$, and $C_{UU}(r,t)=\langle U(R+r,t)U(R,t)\rangle_c$, whose Fourier transforms are the structure functions. The average $\langle\;\rangle$ is over the external noises η and ξ and initial conditions.

Due to the special form of the nonlinear term in the equation of motion, the set of evolution equations for the averages $m(t),U(t)$ and the correlation functions is closed. Indeed, in the Fourier space these read

$$\frac{\partial\phi(\boldsymbol{k},t)}{\partial t} = F_\phi(\boldsymbol{k}) + \eta(\boldsymbol{k},t), \tag{35}$$

$$\frac{\partial U(\boldsymbol{k},t)}{\partial t} = F_U(\boldsymbol{k}) + \xi(\boldsymbol{k},t), \tag{36}$$

where $F_{\phi,U}$ are the Fourier transforms of the first term on the right-hand sides of Eqs. (27) and (28). From Eq. (26) we have

$$F_\phi(\boldsymbol{k}) = M_{\phi\phi}(k,t)\,\phi(\boldsymbol{k},t) + M_{\phi U}(k,t)\,U(\boldsymbol{k},t), \tag{37}$$

$$F_U(\boldsymbol{k}) = M_{U\phi}(k,t)\,\phi(\boldsymbol{k},t) + M_{UU}(k,t)\,U(\boldsymbol{k},t), \tag{38}$$

where the matrix elements are given by

$$\begin{gathered} M_{\phi\phi}(k,t) = -\Gamma_\phi[\xi^2k^2 + r + gm^2(t) + gS(t)],\\ M_{\phi U}(k,t) = \Gamma_\phi\lambda,\quad M_{U\phi}(k,t) = D\lambda k^2,\\ M_{UU}(k,t) = -2D\lambda k^2. \end{gathered} \tag{39}$$

where $r=-g+\lambda/2$ and, in the limit $V\to\infty$, the quantity $S(t)$ is the integrated ϕ-structure function

$$S(t) = \frac{1}{V}\int d^dx\langle\phi(\boldsymbol{x},t)\phi(\boldsymbol{x},t)\rangle - m^2(t) = \sum_k\;\langle\phi(\boldsymbol{k},t)\;\phi(-\boldsymbol{k},t)\rangle_c \tag{40}$$

and $m(t)=\langle\phi\rangle$.

As a consequence, we have

$$\frac{\partial m(t)}{\partial t} = M_{\phi\phi}(0,t)m(t) + M_{\phi U}(0,t)Q(t), \tag{41}$$

$$\frac{\partial Q(t)}{\partial t} = 0, \tag{42}$$

expressing the conserved nature of the field U, and

$$\frac{1}{2}\frac{\partial}{\partial t}C_{\phi\phi}(k,t) = M_{\phi\phi}(k,t)C_{\phi\phi}(k,t) + M_{\phi U}(k,t)C_{\phi U}(k,t) + \Gamma_\phi T_f, \tag{43}$$

$$\frac{\partial}{\partial t}C_{\phi U}(k,t) = M_{U\phi}(k,t)C_{\phi\phi}(k,t) + [M_{UU}(k,t) + M_{\phi\phi}(k,t)]C_{\phi U}(k,t) + M_{\phi U}(k,t)C_{UU}(k,t), \tag{44}$$

$$\frac{1}{2}\frac{\partial}{\partial t}C_{UU}(k,t) = M_{U\phi}(k,t)C_{\phi U}(k,t) + M_{UU}(k,t)C_{UU}(k,t) + DT_fk^2. \tag{45}$$

We note that a closure at the same level would have been obtained in the framework of a Hartree approximation for the model with local constraint described by Eqs. (18) and (19). However, within the present model Eqs. (41)–(45) are exact and not the result of an approximate decoupling of the correlations.

IV. LONG-TIME BEHAVIOR

In this section we shall discuss the behavior of the spherical phase field model for long times, i.e., $t\to\infty$. The results will be compared with those of direct numerical simulation in Sec. V.

We assume that at the initial time we have an undercooled liquid with some supercritical solid seeds. This means that $\overline{u}<0$, while $m=\phi$ lies in the interval (0,1). For a generic initial configuration, the undercooled liquid is not in equilibrium. Thus, at the initial stage the relaxation of the field ϕ is only slightly modified by the dynamics of the slower field U, which can be considered ‘‘almost quenched.’’ During this stage the size of the solid seeds grows with time, while the maximum of the structure function is located at $k=0$ and grows with time. If this regime is long enough, one can recognize a typical nonconserved order parameter dynamics domain growth proportional to $t^{1/2}$.

This kind of behavior persists until the typical size of the domains reaches that associated with the conserved U field. At this time the dynamics of the two fields becomes strongly correlated and the conserved order parameter dynamics eventually dominates. As a consequence, the ϕ field slows down, since the coupling with the conserved U field acts as an additional constraint, while $m(t)$ becomes nearly constant and equal to the asymptotic value, i.e., $m\sim\phi_\infty$.

The crossover time t_c can be readily estimated from dimensional arguments. An inspection of Eqs. (35) and (36) reveals that under a suitable transformation of parameters, in which $\lambda t\rightarrow t$, the dimensionless parameter λ can be traced out.

This means that the crossover time t_c to the conserved dynamics is also of order $\sim 1/\lambda$. It can be shown that the Langevin equations (35) and (36) obey detailed balance [11] and that the stationary probability density is

$$P_{\rm st}[\phi,U]\propto\exp\left(-\frac{1}{T_f}\,\mathcal{F}[\phi,U]\right). \tag{46}$$

Using this we easily get the equilibrium $\phi\phi$ correlation function, which reads

$$\langle\phi\phi\rangle=\frac{T_f}{\xi^2k^2+r+gS+gm^2-\lambda/2}. \tag{47}$$

The appearance of an ordered phase, with $m\neq 0$ for temperatures T_f below the critical temperature T_c, is revealed by the divergence of the $k=0$ mode. This implies that the equilibrium (i.e., when $t\rightarrow\infty$) value of m must satisfy the equation

$$r+gS+gm^2-\lambda/2=0. \tag{48}$$

On the other hand, from the equation of motion (41) m must be the solution of

$$rm+gm^3+gSm-\lambda Q=0. \tag{49}$$

The simultaneous solution of Eqs. (48) and (49) requires

$$m=2Q, \tag{50}$$

which, via Eq. (17) together with $\Delta\phi=2$, implies $\bar{u}=0$. This means that the system relaxes towards a nontrivial phase coexistence state, with nonvanishing order parameter and diverging small-k fluctuations.

One sees that the condition (50) can be satisfied only for $-1/2\leqslant Q\leqslant 1/2$. If Q lies outside this interval the system does not relax to a mixed phase, but instead settles in a spatially uniform state without zero modes. Indeed, in this case $S(t)$ vanishes and m relaxes for long times to the value given by [cf. Eq. (41)]

$$rm+gm^3-\lambda Q=-gm(1-m^2)-\lambda\bar{u}=0. \tag{51}$$

We note that Eq. (51) is equivalent to saying that a spatially uniform field $\phi(x)$ is a stable minimum of the potential $\mathcal{F}$. For large enough values of $|\bar{u}|$ Eq. (51) has a single solution, positive for $\bar{u}>0$ and negative for $\bar{u}<0$. These correspond to a liquid phase above the melting temperature, i.e., positive m and $\bar{u}$, and a solid phase below the melting temperature, i.e., negative m and $\bar{u}$. As $|\bar{u}|$ decreases two additional solutions eventually appear. One of these is unstable while the other represents a metastable spatially uniform state; i.e., solid above the melting temperature $(\bar{u}>0)$ and liquid below the melting temperature $(\bar{u}<0)$. These solutions, however, are unstable against fluctuations; indeed, the presence of $S(t)$, which vanishes only for $t\rightarrow\infty$, prevents the dynamics from reaching these metastable states. Therefore, for any value of $\bar{u}$ the physical solution of Eq. (51) is the most negative one for $\bar{u}<0$ and the most positive one for $\bar{u}>0$. For small $\bar{u}$ we have $m=[1-2(\lambda/g)\bar{u}]\ \mathrm{sgn}\bar{u}$.

A more detailed analysis of the approach to equilibrium can be done by employing a quasilinearization procedure, i.e., we assume that the quantity $R(t)=r+gm(t)^2+gS(t)$ can be treated as a constant, along different pieces of the trajectory [10]. One can verify *a posteriori* that the assumption is valid and leads to useful predictions. Since the behavior at $T_f=0$ is representative of the entire dynamics in the ordered phase when $T_f<T_c$, we also set $T_f=0$, without losing relevant information.

Assuming the quantity $R(t)$ to be nearly constant, Eqs. (33) and (36) become a linear system whose solution has the form

$$\phi(k,t)=c_\phi^+(k)\ e^{\omega_+(k)t}+c_\phi^-(k)\ e^{\omega_-(k)t},$$

$$U(k,t)=c_U^+(k)\ e^{\omega_+(k)t}+c_U^-(k)\ e^{\omega_-(k)t}, \tag{52}$$

where $\omega_+(k)$ and $\omega_-(k)$ are the eigenvalues of the M matrix,

$$\omega_\pm(k)=\frac{1}{2}\{-\Gamma_\phi(\xi^2k^2+R)-2D\lambda k^2 \pm\sqrt{[\Gamma_\phi(\xi^2k^2+R)+2D\lambda k^2]^2+4\,\Gamma_\phi D\lambda^2k^2}\}. \tag{53}$$

For time $t\gg 1$ the dynamical behavior of the solution is determined by the larger eigenvalue $\omega_+(k)$. For large values of k^2 the eigenvalue $\omega_+(k)$ decreases as $-k^2$; thus, to discuss the behavior of the solutions after the initial transient a small-k expansion of $\omega_+(k)$ is sufficient. The form of this expansion depends on the sign of $R(t)$. When $R(t)$ is negative the appropriate expansion of $\omega_+(k)$ is

$$\omega_+(k)=\Gamma_\phi|R|-\left[\Gamma_\phi\xi^2-D\frac{\lambda^2}{|R|}\right]k^2. \tag{54}$$

Notice that in the regime where Eq. (54) is valid there is a competition between the curvature term $\Gamma_\phi\xi^2$, which represents the driving force of the dynamics of the pure model A, and the term $D\lambda^2/|R|$ due to the coupling to the heat diffusion. For $R(t)>0$, the representation Eq. (54) breaks down and one must instead consider the expansion

$$\omega_+(k)=2D\lambda\left(\frac{\lambda}{2R}-1\right)k^2-c_4k^4, \tag{55}$$

where c_4 is a positive coefficient.

Since the value of $R(t)$ as well as its sign changes along the trajectory, one must employ either Eq. (54) or (55), depending on the stage of the growth process. On the other hand, this kind of analysis is not applicable in the crossover region where $m(t)$ and $S(t)$ vary too rapidly and $R(t)\sim 0$, but this fact does not invalidate our findings.

All the relevant behaviors can be classified according to the value of the conserved field Q. To this purpose one must treat separately the cases $Q>0$ and $Q<0$.

Let us consider first the case $Q<0$ and assume $m(t=0)\sim 1$, i.e., the system initially is formed by an undercooled liquid. In the initial stage the fields ϕ and U are nearly uniform and characterized by small fluctuations. In the evolution equation for m, U plays the role of a constant field of value Q; hence

$$\frac{\partial m}{\partial t} = -\Gamma_\phi\,[R(t)m(t)-\lambda Q] \tag{56}$$

describes the relaxation of m in a static field Q. During such a stage the system relaxes towards the nearest fixed point that makes the right-hand side of Eq. (56) vanish. Equating to zero $\partial m/\partial t$ we get the relation

$$R(t)=\lambda\frac{Q}{m}, \tag{57}$$

which is negative for $m>0$ and $Q<0$, so that the relevant expansion is Eq. (54). Thus the liquid phase is unstable, as can be seen from Eq. (54); in fact, as long as $m(t)$ remains positive the system develops strong fluctuations about the uniform mode $k=0$. Such a regime lasts for a time of order $t_c\sim 1/\lambda$, after which the fluctuations eventually drive the system towards negative values of the order parameter so as to reduce the free-energy cost.

In the successive stage the system becomes prevalently solid, which is signaled by the change of sign of m. Also R changes sign, so the expansions (54) becomes invalid. However, for times $t \gg 1/\lambda$, long after the transition, the evolution of m slows down again, i.e., $\partial m/\partial t \simeq 0$ and $R>0$, so that Eq. (55) is appropriate. Using the result (57), the relevant form of $\omega_+(k)$ is

$$\omega_+(k)=D\lambda\left(\frac{m}{2Q}-1\right)k^2-c_4k^4. \tag{58}$$

Such expression shows that whenever $m/2Q<1$, all modes of finite wave vector are damped and one cannot observe growing modes: the system relaxes towards a spatially uniform state.

On the other hand, if $m/2Q>1$ fluctuations are large up to a finite wave vector, because the fastest growing mode is located at a finite k. This case corresponds to a phase that is spatially nonuniform with large fluctuations. Asymptotically, $m=2Q$ and the peak position k_m moves towards vanishing values of k. This scenario is typical of the conserved order parameter dynamics. Indeed, as done in Refs. [10,11], it can be shown that in this regime the dynamics exhibits multiscaling [10].

In Fig. 1 we report the behavior of $\partial m/\partial t$ versus the order parameter m. For small negative values of λQ, $\partial m/\partial t$ nearly touches the horizontal axis and the evolution of m becomes very slow.

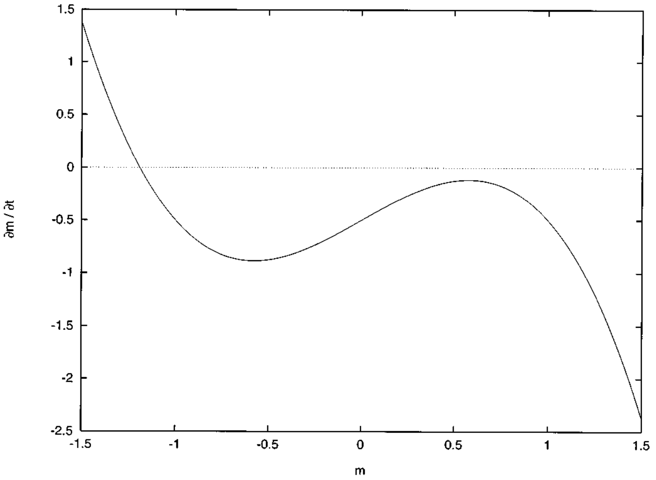

FIG. 1. Schematic behavior of $\partial m/\partial t$ as a function of m, from Eq. (56).

Let us now turn to the $Q>0$ case. In this case, from Eq. (57) it follows that $R(t)>0$, so that the relevant expansion is Eq. (58). In analogy with the $Q<0$ case, from Eq. (58) we conclude that if $Q>1/2$, the phase $m\sim 1$ is stable, and the final state is pure, i.e., it is characterized by small spatial fluctuations.

For smaller values of Q, i.e., $0<Q<1/2$, the coefficient of the term of order k^2 of the eigenvalue ω_+ is positive and the peak of $C_{\phi\phi}(k,t)$ is located at a finite wave vector. This causes an instability of the initial pure phase $m\sim 1$ and the appearance of a mixed phase, characterized by a lower, but still positive, value of $m(t)$.

V. NUMERICAL RESULTS

In what follows we shall consider the zero-temperature dynamics because it is known to be representative of the subcritical behavior. We have compared the numerical results with the predictions of the preceding section and found good agreement.

We have solved numerically the equations of motion (35) and (36) in two dimensions by using a simple Euler second-order algorithm and a discretization of the integrals on an $N\times N$ bidimensional lattice. We used periodic boundary conditions. The parameters employed are

$$\xi=1,\quad g=1/2\epsilon^2,\quad \lambda=4\Lambda/\epsilon^2,$$

$$\Gamma_\phi=1/\alpha,\quad D=\epsilon^2/8\Lambda, \tag{59}$$

with $\epsilon=0.005$, $\Lambda=0.1$, and $\alpha=10$. The time step used is $\Delta t=2\times 10^{-5}$ and a lattice space $\delta x=0.01$. Different values of N were used; here we report the results for $N=256$.

The system was initially prepared in a nonuniform initial state formed by 70% of undercooled liquid and the remaining 30% of seeds of solid randomly distributed. This ensures that at the initial time the order parameter $m(t=0)$ is positive and the correlations are small. As long as these two conditions are met, the results are not too sensitive to the

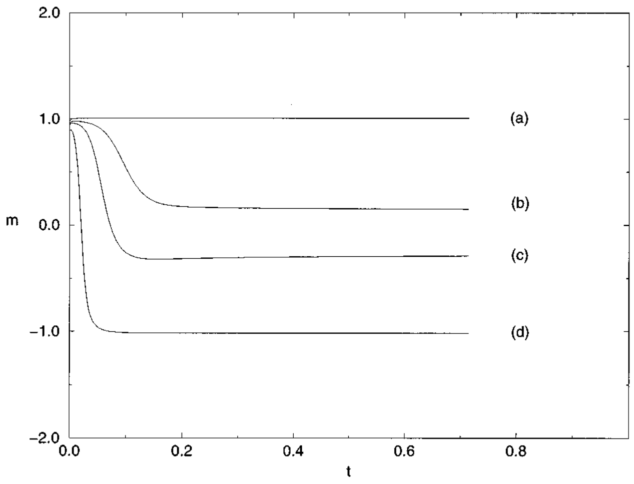

FIG. 2. Typical behaviors of the order parameter m as a function of time for (a) $Q>1/2$, (b) $0<Q<1/2$, (c) $-1/2<Q<0$, and (d) $Q<-1/2$. In all runs shown here we started with $m(t=0)=0.54$, while the other parameter were (a) $\overline{u(t=0)}=0.4$, $Q=0.67$, $m(\infty)\neq 2Q$; (b) $\overline{u(t=0)}=-0.2$, $Q=0.07$, $m(\infty)=2Q$; (c) $\overline{u(t=0)}=-0.4$, $Q=-0.13$, $m(\infty)=2Q$; and (d) $\overline{u(t=0)}=-1.0$, $Q=-0.73$, $m(\infty)\neq 2Q$.

initial solid-liquid fraction. The thermal field u was taken to be uniform, $u_{ij}(t=0)=\overline{u(t=0)}$, with both positive and negative values. According to Eq. (17), the conserved field U was chosen to be equal to

$$U_{ij}(t=0)=\overline{u(t=0)}+\frac{1}{2}\,\phi_{ij}(t=0). \tag{60}$$

The model exhibits two different long-time regimes as far as the temperature field is concerned. The snapshots of the field ϕ indeed reveal that changing from positive values of the conserved field Q to negative values the long-time morphology changes. For $Q>0$ one observes solid drops immersed in a liquid and $u\leqslant 0$, whereas for $Q<0$ liquid drops become trapped in a solid matrix and $u\geqslant 0$. This is in agreement with the general results of thermodynamics. For quenches with positive Q the minority phase is the solid, thus we expect the solid drops to have positive curvature. Indeed, relating the curvature $\mathcal{K}$ to the temperature field, we obtain from the Gibbs-Thompson condition $u=-d_0\mathcal{K}$ [7] a negative value of u for $Q>0$. On the contrary, upon crossing the $Q=0$ line, the solid becomes the majority phase and u changes sign since the curvature relative to the solid is negative.

In Fig. 2 we show the behavior of the order parameter m as a function of time for the four distinct regimes. In all cases at the initial time we have $m=0.54$. We note that in the case $|Q|>1/2$ the system evolves towards a spatially uniform state, which is a liquid above the melting temperature for $Q>1/2$ and positive initial $\overline{u(t=0)}$ [case (a) in the figure] or a solid below the melting temperature for $Q<1/2$ and negative initial $\overline{u(t=0)}$ [case (d) in the figure]. This state minimizes the potential $\mathcal{F}$. In the case $|Q|<1/2$ the system evolves towards a phase equilibrium state at the melting temperature: we have for $t\to\infty$, $u=\overline{u}=0$ and $m=2Q$, in agreement with the analytical results of Sec. IV.

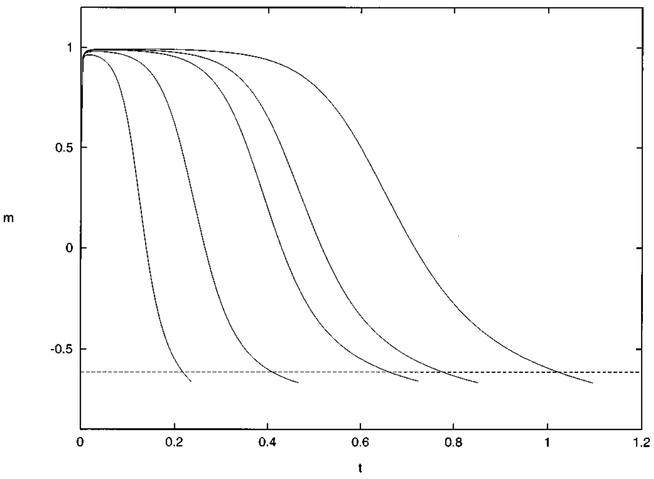

FIG. 3. Order parameter m as a function of time for $Q=-0.3077$ and different values of λ; from right to left $\lambda=128,170,200,300,500$. The plateau increases as λ decreases. Initially the parameters are $m=0.385$ and $u=-0.5$. The dashed line denotes the value $2Q$.

When the system starts from an undercooled state, i.e., $u<0$ at the initial time [cases (b)–(d) in Fig. 2], despite the fact that the liquid state is unfavorable, m increases for short times. The system then evolves towards a liquid state, m tends to saturate to a fixed value ~ 1, and the fluctuations are small. This state is, however, unstable with respect to fluctuations, and indeed after a time t_c we observe a transition towards the asymptotically stable state, which depends on the value of $Q<1/2$.

The time t_c is a decreasing function of λ, as can be seen in Fig. 3, where we report m as a function of time for $-1/2<Q<0$ and various values of λ. In Fig. 4 we report t_c versus λ for the curves of Fig. 3. The line is the theoretical prediction $t_c\sim 1/\lambda$. In this figure we define t_c as the time such that $\min_t m(t)=2Q$. Other definitions are possible, for example, when $m(t)=0$ or any other fixed value. All these definitions leads to the same scaling with λ.

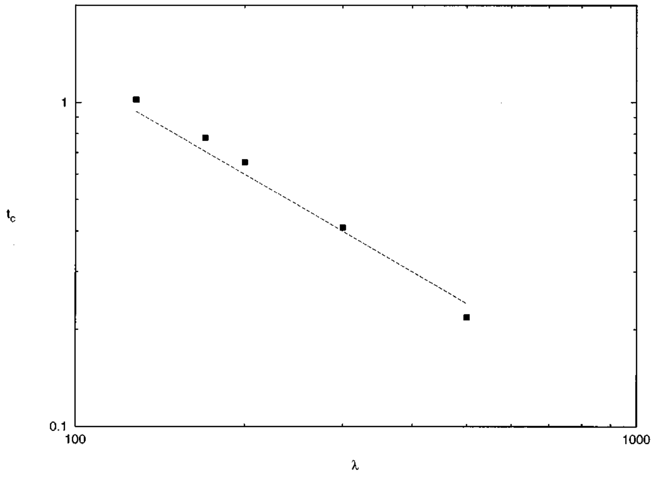

FIG. 4. Crossover time t_c as a function of λ for the curves of Fig. 3. The dashed line is the scaling $1/\lambda$. The crossover time is defined as $\min_t m(t)=2Q$.

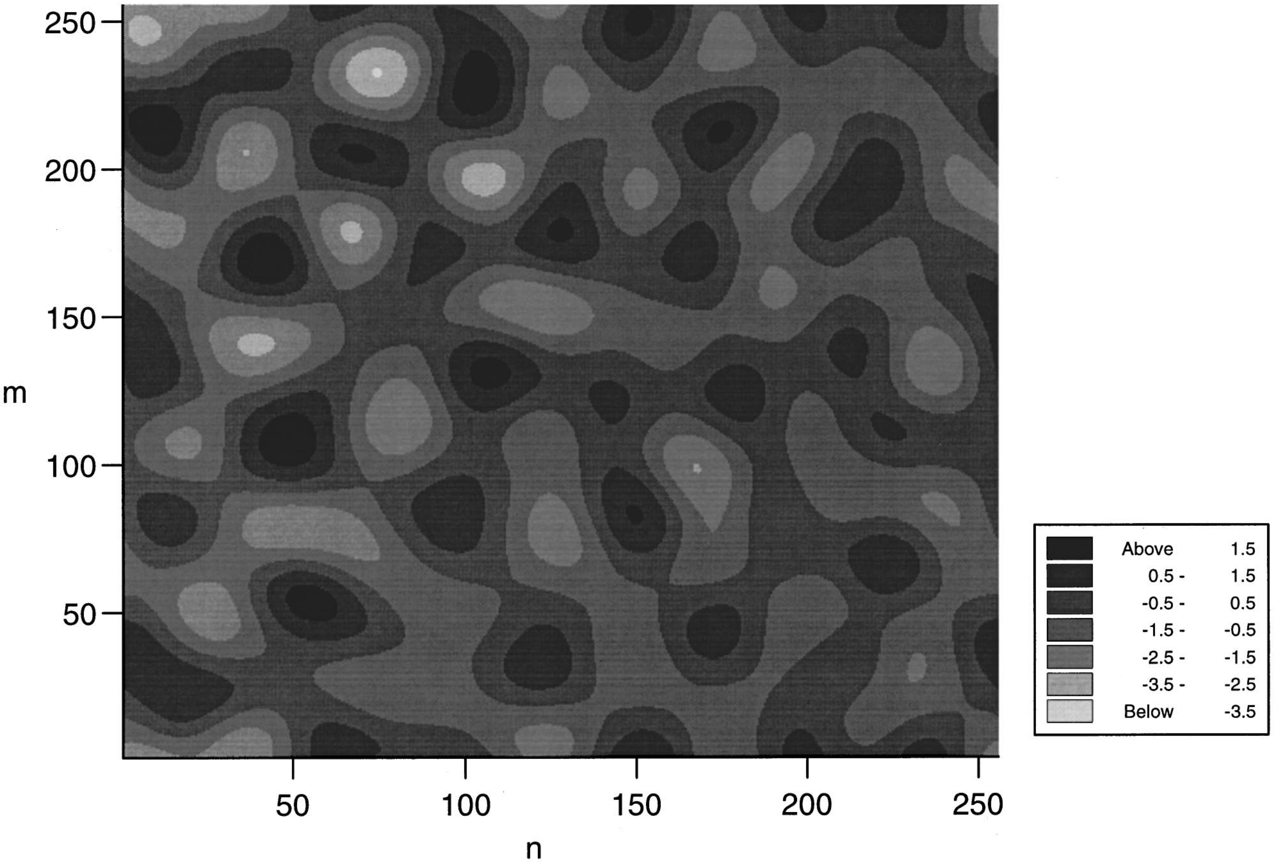

FIG. 5. Snapshot of the ϕ field for the global constraint case and $-1/2<Q<0$. The lattice index is reported on the axis.

The scenario depicted here remains valid also for the local constraint case. This has been checked by numerically integrating the appropriate equations. The main difference between the local and the global case shows up at the morphological level, as can be seen in the snapshots of Figs. 5 and 6. As one can see, while the phase field model with local constraint has a sharp domain wall, the model with the global constraint presents smoother interfaces. We stress that despite this difference the circularly averaged correlation functions and the structure factors for the two cases are quite similar. In Figs. 7 (global) and 8 (local) we report the circularly averaged $\phi\phi$ correlation for the situations of Figs. 5 and 6 (circles), as well as for the case $|Q|>1/2$ (diamonds). The average radius of the drops is identified by the first zero of correlation functions.

While the simulations confirm the scenario described in Sec. IV, we cannot extract the power-law exponent predicted by the nonconserved ordered parameter dynamics at short times, as well as those of the conserved order parameter dynamics for long times. Indeed, finite-size effects prevent us from reaching the conserved regime.

CONCLUSION

We have studied a model that reproduces many of the features that render appealing the scalar phase field model and analyzed its equilibrium and off-equilibrium properties. We transformed the original scalar model into a model with global couplings, which is more amenable to analytic investigations.

In such a description the temperature shift from the coexistence temperature plays the role of an annealed field, which changes during the process and settles to a value determined by energetic considerations. Its dynamics are slow compared to that of the order parameter field and the latter becomes eventually slaved by the first.

The long-time state can be either a pure state with vanishing correlations, in the limit $T_f=0$, or a mixed state with large spatial fluctuations in the order parameter. The type of equilibrium reached depends on the initial value of the spatial average Q of the field U. Indeed, in the case $-1/2<Q<1/2$, the system shows a tendency towards separation into two phases in proportions given by the rule $m=2Q$ and one observes drops of the minority phase in a sea formed by the majority phase. At the same time the thermal field u vanishes, indicating that $T=T_M$ in the whole volume. The number of the drops decreases with time to minimize the free energy of the system, but for long times the total amount of solid remains fixed because the heat released by a growing solid drop can only be adsorbed by a shrinking solid drop. As a result, the solid order parameter ϕ becomes nearly conserved, being mediated by the conserved heat field. At this stage the dynamics of the crystalline order parameter becomes a genuine conserved order parameter dynamics. One can, in fact, observe multiscaling if the volume of the systems is large enough. The existence of inhomogeneous structures is mirrored in the presence of the peak in the structure factor at finite wavelength and the phenomenon is similar to the Ostwald ripening. The undercooling initially present is not sufficient to promote the transfor-

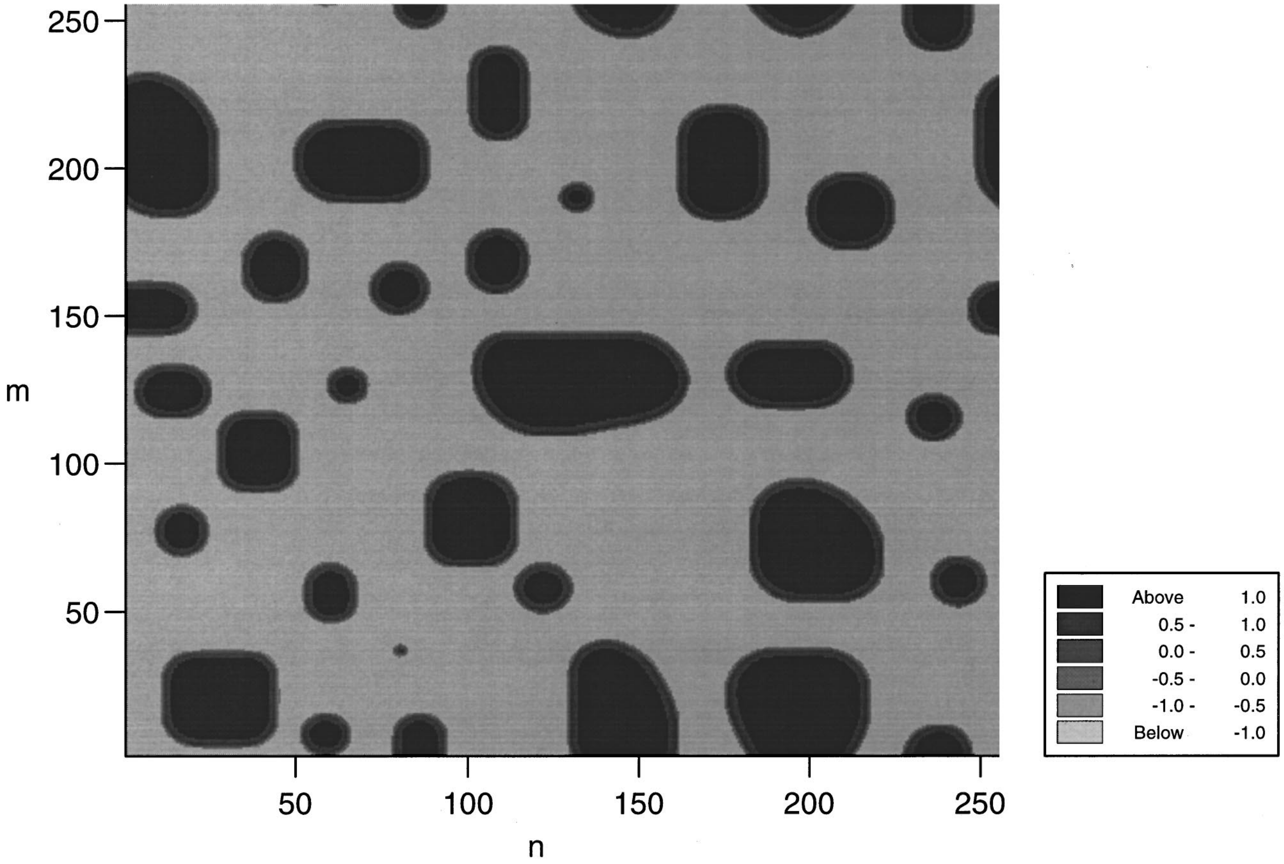

FIG. 6. Snapshot of the ϕ field for the local constraint case and $-1/2<Q<0$. The lattice index is reported on the axis.

mation of all the liquid into the solid state, and some drops of either phase remain trapped into the other.

To summarize the results we have established the following rules governing the evolution.

(i) The field U is constant in time.

(ii) The order parameter $m(t)$ as $t\to\infty$ tends to the asymptotic value $m=2Q$, if Q falls in the range $[-1/2,1/2]$. This fact in turn implies that the spatial average value of u over the system vanishes as $t\to 0$, i.e., the system reaches two-phase coexistence asymptotically.

(iii) In the above range of Q, the correlation function is large and centered at finite values of the wave vector k.

(iv) If $|Q|$ exceeds the threshold value 1/2 the system evolves towards a spatially uniform state with $m\sim -1$ and vanishing correlations and m is no longer equal to $2Q$. In this case u reaches an equilibrium value that is nonzero and the system is out of two-phase coexistence.

(v) Therefore, larger values of the undercooling cause the

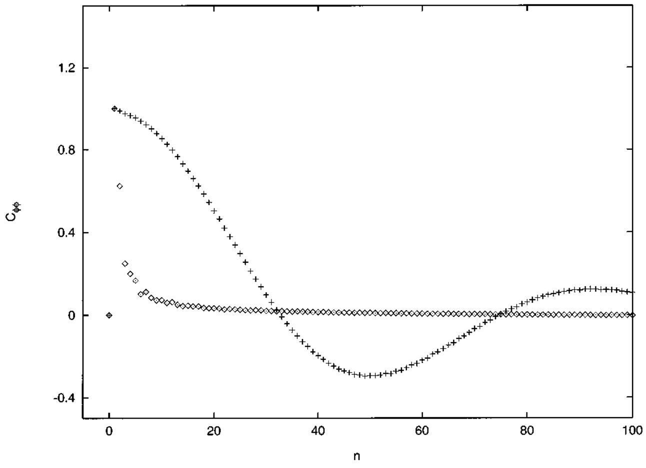

FIG. 7. Circularly averaged $\phi\phi$ correlation function as a function of the lattice index for the global constraint case obtained numerically: circles represent $|Q|<1/2$ and diamonds refer to $|Q|>1/2$.

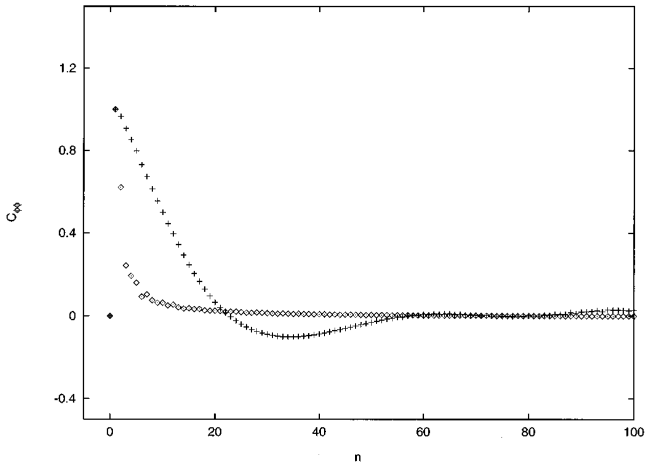

FIG. 8. Circularly averaged $\phi\phi$ correlation function as a function of the lattice index for the local constraint case obtained numerically: circles refer to $|Q|<1/2$ and diamonds represent $|Q|>1/2$.

melt to crystallize completely and thus correlations are asymptotically suppressed as the system reaches an homogeneous state.

The above features are interesting because they mimic the behavior of the more realistic phase field model with local constraint.

We finally remark that perhaps the most serious flaw of the model is that it suffers from the same problem as the spherical model. In contrast to the local constrained phase field model, which displays a region of metastability of the liquid phase in the ϕ-T plane, between the coexistence line and the spinodal line [27], the globally constrained model is always unstable inside the two-phase coexistence line. As a consequence, no nucleation barrier needs to be overcome in the transformation from liquid to solid. In the initial state long-wavelength fluctuations grow and the system becomes unstable. The nucleation barrier is proportional to the surface tension associated with the creation of a kink in the scalar model, whereas in the model with global couplings the energy gaps between the ordered phase and the instanton solutions, i.e., the uniform solutions of the equation, vanish in the infinite volume limit. Thus the mechanism described is non-Arrhenius-like. This is also reflected in the absence of true phase separation since the width of a domain wall diverges in the limit of a vanishing pinning field h as $h^{-1/2}$ [23].

[1] A.J. Bray, Adv. Phys. **43**, 357 (1994).

[2] R. Glauber, J. Math. Phys. (N.Y.) **4**, 294 (1963).

[3] J.W. Cahn and J.E. Hilliard, J. Chem. Phys. **28**, 258 (1958).

[4] P. Hohenberg and B.I. Halperin, Rev. Mod. Phys. **49**, 435 (1977).

[5] J.D. Gunton, M. San Miguel, and P.S. Sahni, in *Phase Transitions and Critical Phenomena*, edited by C. Domb and J.L. Lebowitz (Academic, New York, 1983), Vol. 8, p. 267.

[6] J.S. Langer, Rev. Mod. Phys. **52**, 1 (1980); Science **243**, 1150 (1989).

[7] For comprehensive reviews, see *Dynamics of Curved Fronts*, edited by P. Pelcé (Academic, New York, 1988); *Solids Far From Equilibrium*, edited by C. Godrèche (Cambridge University Press, Cambridge, 1992).

[8] W.L. Mullins and R.F. Sekerka, J. Appl. Phys. **35**, 444 (1964).

[9] H. Müller-Krumbahaar and W. Kurz, in *Materials Science and Technology*, edited by R.W. Cahn, P. Haasen, and E.J. Kramer (VCH, Weinheim, 1991), Vol. 5.

[10] U. Marini Bettolo Marconi and A. Crisanti, Phys. Rev. Lett. **75**, 2168 (1995).

[11] U. Marini Bettolo Marconi and A. Crisanti, Phys. Rev. E **54**, 153 (1996).

[12] M. Conti, F. Marinozzi, and U. Marini Bettolo Marconi, Europhys. Lett. **36**, 431 (1996).

[13] J.B. Collins, A. Chakrabarti, and J.D. Gunton, Phys. Rev. B **39**, 1506 (1988).

[14] P. Keblinski, A. Maritan, F. Toigo, and J.R. Banavar, Phys. Rev. E **49**, R4795 (1994); Phys. Rev. Lett. **74**, 1783 (1995).

[15] O. Penrose and P. Fife, Physica D **69**, 107 (1993).

[16] S.L. Wang, R.F. Sekerka, A.A. Wheeler, B.T. Murray, S.R. Corriel, R.J. Braun, and G.B. McFadden, Physica D **69**, 189 (1993).

[17] R. Kupferman, O. Shochet, E. Ben-Jacob, and Z. Schuss, Phys. Rev. B **46**, 16 045 (1992).

[18] The model has been introduced in a slightly different form by T.H. Berlin and M. Kac, Phys. Rev. **86**, 821 (1952).

[19] A recent reference about the dynamics of $O(n)$ models is A. Coniglio, P. Ruggiero, and M. Zannetti, Phys. Rev. E **50**, 1046 (1994).

[20] S. Ciuchi, F. de Pasquale, P. Monachesi, and B. Spagnolo, Phys. Scr. **T25**, 156 (1989).

[21] The present spherical model defined by Eq. (26) is different from the $O(n)$ spherical model discussed in previous papers [11]. In that case both the order parameter and the U field were vector fields coupled bilinearly. However, the two models in the infinite-volume limit and in the limit of infinite components generate identical equations for the average fields and their correlations, although the physical interpretation remains different for the two models.

[22] Stanley has shown the equivalence of the spherical model and an n-component spin model in the limit of $n \rightarrow \infty$ in the case of translationally invariant systems. H.E. Stanley, Phys. Rev. **76**, 718 (1968).

[23] D.B. Abraham and M.A. Robert, J. Phys. A **13**, 2229 (1980).

[24] J. Weeks, J. Chem. Phys. **67**, 1306 (1977).

[25] The equilibrium properties of interfaces have been studied in the mode-coupling approximation by U. Marini Bettolo Marconi and B.L. Gyorffy, Physica A **159**, 221 (1989); Phys. Rev. A **41**, 6732 (1990).

[26] Notice that the values of the coupling parameters of the U^2 term and $U\phi$ in Eq. (26) have not been chosen independently, as assumed in Ref. [11], but their ratio was fixed to guarantee the correct energy balance as explained in Secs. II and I.

[27] Although the notion of a spinodal line signaling a sharp transition from a nucleation mechanism to a spinodal decomposition mechanism is not exact in systems with finite-range interactions and the transition is gradual, still the concept of spinodal has a heuristic value [see, for example, the article by Binder about spinodal decomposition: K. Binder, in *Materials Science and Technology*, edited by R.W. Cahn, P. Haasen, and E.J. Kramer (VCH, Weinheim, 1991)].